Revue Roumaine de Chimie, **2007**, *52*(12), 1123–1130

THE CATHODIC EVOLUTION OF HYDROGEN ON NICKEL IN ARTIFICIAL SEAWATER

Gabriela Elena BADEA,[a] Ioana MAIOR,[b*] Anca COJOCARU [b] and Ion CORBU[c]

[a] Department of Thermal Energy, University of Oradea, Str. Universităţii 1, 410087, Oradea, Roumania
[b] Deparment of Appl. Phys. Chem and Electrochem., "Politehnica" University of Bucharest, Calea Griviţei 132, 010737, Bucharest, Roumania
[c] Roumanian American University of Bucharest, Expozitiei Bd. 1B, 012101, Bucharest, Roumania

Received September 26, 2006

The hydrogen evolution reaction (HER) on Ni electrode in artificial seawater was investigated by steady-state polarisation curves and electrochemical impedance spectroscopy methods at the room temperature and at high temperatures (30–60°C). The electrochemical kinetics parameters of the HER – Tafel slope, charge transfer coefficient and exchange current density – were evaluated in accordance with the potential scan direction and temperature. The Tafel slopes are significantly higher than 120 mV/decade and they increase with the increasing of the solution temperature. The charge transfer coefficient is lower than 0.5 and it decreases with temperature. The exchange current density has a magnitude order of 10^{-5} A·cm^{-2} and its value is increasing with increasing solution temperature. The activation energy of the HER has a moderate value, that slowly decreases with the cathodic polarisation increase. The HER is controlled by the charge transfer step and by the mass transfer of the intermediate reaction product H_{ads} on the electrode surface.

INTRODUCTION

The seawater electrolysis is now used for various applications: NaClO generation for to water disinfection, elimination of plankton from seawater, sterilisation of wastewater, oxidation of various industrial wastewaters, etc. Regarding the necessity of alternative power sources development, in recent studies researchers are concerned in obtaining electrical energy from marine waves and using it *in situ* for hydrogen generation by seawater electrolysis.

Nickel is a metal widely applied as the cathodic material in water electrolysis, due to its good catalytic activity and stability in alkaline media[1] and also in neutral solutions, even in seawater[2].

Recently, many studies were concerned in hydrogen evolution reaction (HER) on nickel, nickel alloys, Ni–P–titanium oxide electrodes in alkaline[3-14] and acid[15] solutions.

About the reaction mechanism, in alkaline solutions, the mainstream opinion is that atomic hydrogen is an intermediate product, the HER following the scheme:[3, 5, 8, 10-12]

$$H_2O + M + e^- = MH_{ads} + OH^- \qquad \textit{Volmer step} \qquad (1)$$

$$MH_{ads} + H_2O + e^- = H_2 + M + OH^- \qquad \textit{Heyrovsky step} \qquad (2)$$

$$2MH_{ads} = H_2 + 2M \qquad \textit{Tafel step} \qquad (3)$$

$$MH_{ads} \rightarrow MH_{ads}\bullet \qquad (4)$$

* Corresponding author: i_maior@chim.upb.ro

The Volmer step (reaction 1) is the primary electron transfer step with formation of adsorbed hydrogen on the electrode surface (MH_{ads}) from H_2O molecule. It is followed by the Heyrovsky step or/and the Tafel step with the formation of H_2 molecule. The occurrence of Heyrovsky step (reaction 2) suggests the formation of H_2 molecule by desorption of adsorbed hydrogen and a simultaneous reduction of H_2O molecule. The Tafel step (reaction 3) suggests the formation of H_2 molecule by a combination of two neighbouring adsorbed hydrogen atoms. A fraction of atomic hydrogen (H_{ads}.) may undergo adsorption in a surface layer of nickel, thus altering its catalytic properties.[16]

The proposed mechanisms for the HER in literature are combinations of Volmer and Tafel steps or of Volmer and Heyrovsky steps with one step as rate controlling.

Krstajić *et al.*[3] have studied mechanism and kinetics of the HER in 1 M NaOH by steady-state polarisation curves and impedance spectroscopy. In the potential region – 0.95 ÷ 1.1 V/SHE, they found that the mechanism of the HER is a consecutive combination of the Volmer step, followed dominantly by a rate controlling Tafel step, while the contribution of the parallel Heyrovsky step is negligible. At potential more negative than –1.2 V/SHE, the mechanism of HER is consecutive combination of the Volmer step, followed by a Heyrovsky step, while the contribution of the Tafel step is negligible.

Chen and Lasia[10], Spătaru *et al.*[11] and Notoya[12] have considered that HER on Ni and Ni alloys proceeds via Volmer – Heyrovsky mechanism with the Volmer reaction as the rate-determining step.

Kreysa *et al.*[13] using experimental steady-state polarisation curves have analysed the kinetics of the HER on polycrystalline and amorphous nickel electrode and have calculated the values of rate constants for the three steps. They observed a limiting current for HER at high current densities (close to 1 $A \cdot cm^{-2}$). Considering the Volmer–Tafel mechanism, they assumed that this limiting current is caused by the Tafel step as the *rds* due to the relatively slow surface diffusion of H_{ads} atoms.

Diard *et al.*[14] analysing the HER on Ni in alkaline solution by impedance spectroscopy concluded that the appearance of the inductive component in the low frequency range in impedance diagrams is in good agreement to the corresponding theoretical diagrams for the Volmer– Heyrovsky mechanism.

In spite of many studies of the HER on Ni and other electrodes in acidic or alkaline solutions, we did not find any studies in seawater. The composition of the seawater is substantially the same everywhere, the variations referring to the ratio of water to total salt content. In the laboratory researches the artificial seawater used is based on about 35400 ppm TDS (total dissolved solids), from which about 25000 ppm is taken as NaCl (Table 1).

This paper presents the investigation of kinetics of the hydrogen evolution reaction on Ni electrode in artificial seawater, using the classical steady-state polarisation curves and electrochemical impedance spectroscopy. The temperature effect on steady-state polarisation curves is also investigated.

EXPERIMENTAL

The working electrode was a sheet of nickel of 99.9% purity with active area of 2 cm^2. Specimens were polished successively with 1000 and 1200-grade emery paper, washed with carbon tetrachloride, followed by pickling for 1 minute in a solution containing 3% HCl and washing with distilled water. A standard activation was adopted for all specimens consisting in a cathodic polarisation at –1.2 V/SCE for 1 minute in the studied solution.

A conventional three-compartment glass cell was used. A platinum plate with active area of 4 cm^2 was used as anode. A saturated calomel reference electrode was placed close to the cathode through a Luggin capillary.

The artificial seawater was prepared using chemically pure reagents and double distilled water. The composition of artificial seawater, according to ASTM, is presented in Table 1. The solution has the conductivity of 0.052 $\Omega^{-1} \cdot cm^{-1}$ at 25°C.

Table 1

Artificial seawater composition[17] (according to ASTM D1141)

Chemical compounds	Concentration, g/L	Chemical compounds	Concentration, g/L
NaCl	24.530	$NaHCO_3$	0.201
$MgCl_2.6H_2O$	11.103	KBr	0.101
$Na_2SO_4.10H_2O$	9.278	H_3BO_3	0.027
$CaCl_2.2H_2O$	1.539	$SrCl_2.6H_2O$	0.042
KCl	0.695	NaF	0.003

Quasi-stationary potentiostatic curves were recorded with PS 2 potentiostat, by scanning the electrode potential with 30 mV steps after 1 min. As the current reached about 100 mA, the direction of potential was reversed (backward scan). This technique of measurement was used only at temperature of 25°C.

Table 2

The values of pH in artificial seawater at various temperatures and the corresponding calculated values of the equilibrium potential, E_e, for the HER

T, K	293	303	313	323	333
pH	6.6	6.5	6.4	6.3	6.2
E_e, V/SCE	-0.624	-0.631	-0.638	-0.644	-0.650

The effect of the temperature was studied by recording the steady-state polarisation curves of Ni (forward scan) in the Tafel potential range, from –1.2 to –1.5 V/SCE. In all experiments only the compartments of the working and counter electrodes were thermostated at: 20, 30, 40, 50 and 60°C, respectively. The reference electrode was held constantly at 25°C. The values of the equilibrium potential for the HER, together with the pH of the solution at the above-mentioned temperatures were determined and presented in Table 2. The data obtained from these polarisation curves were used to estimate the energies of activation for the HER at various electrode potentials.

The ac impedance measurements were carried out with Bas-Zahner IM6e potentiostat, controlled by a computer. A Zview software was used to obtain the real (Z_{Re}) and imaginary (Z_{imag}) components of the Ni cathode impedance at each frequency used. So, both impedance spectra in the complex plane (Nyquist diagrams) and the corresponding Bode diagrams were obtained in the frequency range from 30 mHz to 50 kHz, at the following constant potentials: open circuit potential after cathodic activation of Ni, –1.2 and –1.3 V/SCE.

RESULTS AND DISCUSION

The cathodic polarisation curves, obtained on Ni electrode at the temperature of 25°C in artificial seawater at forward and backward scan of the potential, are shown in Fig. 1. As can see, up to –1.2 V/SCE, the curves overlap perfectly, and a depolarisation appears at more negative potentials on backward (curve 2).

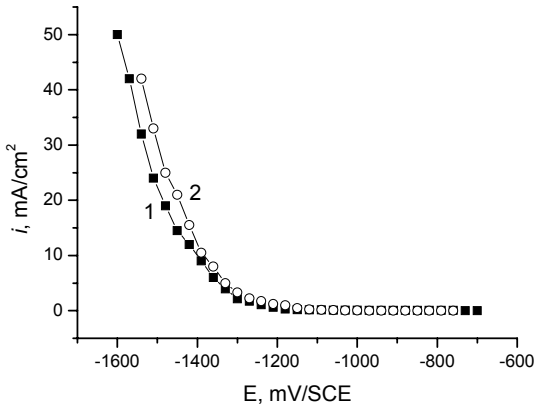

Fig. 1 – Polarisation curves for the HER from artificial seawater on Ni electrode at 25°C: 1 – forward scan; 2 – backward scan of potential.

Fig. 2 shows the corresponding Tafel lines by plotting in semi-logarithmic coordinates. In the Tafel range (*i.e.* $|E - E_e| << -RT/F$), the kinetic equation is given by the expression:

$$i = i_0 \exp\left(-\frac{\alpha \cdot z \cdot F}{R \cdot T} \cdot \eta\right) \qquad (5)$$

where: i – current density corresponding to overpotential $\eta = (E - E_e)$, E – the electrode potential, E_e – the equilibrium potential of HER, i_0 – the exchange-current density and α – the charge transfer coefficient.

By extrapolation of Tafel lines (Fig. 2) to the HER equilibrium potential, i_0 is evaluated, and from the Tafel slope (b) the value of α is obtained.

Although the Tafel slope is expected to be ~120 mV/decade assuming $\alpha \approx 0.5$, large deviations from this value are reported in the literature[13] even in alkaline solutions. In the present study also, the b values obtained are higher than 120 mV/dec. (Fig. 2) and the corresponding values of the charge transfer coefficients are $\alpha_1 = 0.212$ and $\alpha_2 = 0.229$.

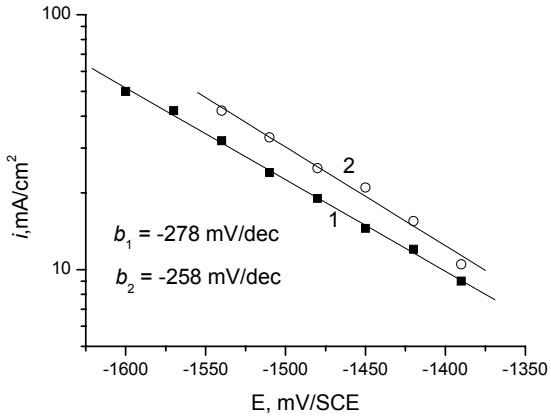

Fig. 2 – Tafel lines for the HER on Ni electrode in artificial seawater at 25°C:
1 – forward scan; 2 – backward scan of potential.

The values of the exchange current density are: $i_{0,1} = 2.05x10^{-5}$ and $i_{0,2} = 7.62x10^{-6}$ A/cm^2, that are similar in magnitude to the reported values for the HER on several electrodes in alkaline electrolytes.[7, 10-12] The value lower with one magnitude order at backward scan of potential indicates the diminution of the electrocatalytic properties of the metal surface by the adsorbed hydrogen on Ni, according to reaction (4).[16]

Fig. 3 shows the polarisation curves for the HER within Tafel potential region on Ni in artificial seawater at various temperatures. In Tab. 3 are given the corresponding kinetics parameters: Tafel slope, b, charge transfer coefficient, α, and exchange current density, i_0.

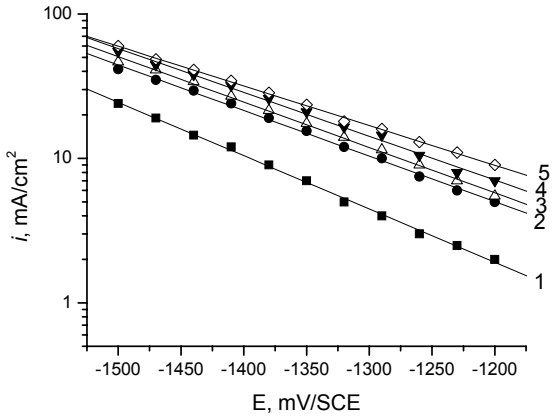

Fig. 3 – Potentiostatic polarisation curves of the HER on Ni in artificial seawater in the Tafel potential region at the following temperatures: 1 – 293; 2 – 303; 3 – 313; 4 – 323; 5 – 333 K.

It can be seen from Fig. 3 that the current densities, at constant potential, increases with the solution temperature and tend to be closer at high cathodic polarisation. Similar behaviour was reported by Krstajić *et al.*[4] who studied the temperature effect on the HER on Ni in alkaline solutions. These authors obtained a limiting current density independent of the temperature in the extended potential region (to approximately –1.8 V/SHE).

Table 3

Electrochemical kinetics parameters of HER on Ni in artificial seawater at various temperatures

T, K	293	303	313	323	333
b, mV/dec.	-271	-317	-318	-328	-363
α	0.214	0.189	0.194	0.195	0.182
i_0*10^5, A/cm^2	1.46	9.1	9.99	14.61	27.89

The Tafel slope values increase with temperature as was expected, whereas the charge transfer coefficient decreases (Tab. 3). The dependence of α with temperature (T) can be approximated by the linear relation (Fig. 4), suggested by Conway:[18]

$$\alpha = \alpha_H + \alpha_S T^{-1} \quad (6)$$

where α_H and α_S are the "enthalpic" and "entropic" components, respectively.

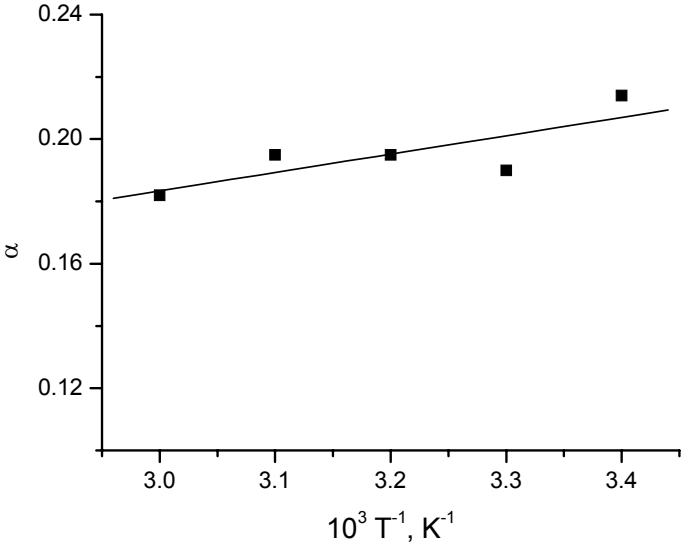

Fig. 4 – Conway plot of the temperature dependence of the experimental transfer coefficient for HER on Ni electrode in artificial seawater.

We have noticed that the exchange current density (i_0) of the HER significantly increases with temperature (Tab. 3). Thus, at the temperature of 333 K, i_0 value is about 20 times higher than that obtained at 293 K.

Fig. 5 shows the Arrhenius plot, log i – 1/T, at three selected electrode potentials in the range of more negative values than −1350 mV/SCE. The values of the activation energies (Q) for the HER in artificial seawater, together with the corresponding pre-exponential term (A) from Arrhenius equation are given in Table 4.

In the studied potential region, the activation energy of the HER has a moderate value, which slowly decrease by shifting the potential towards negative values. According to Krstajić *et al.*[4] a low activation energy for HER is consistent with a mechanism composed of consecutive Volmer and Tafel steps with the Tafel step as rate determining.

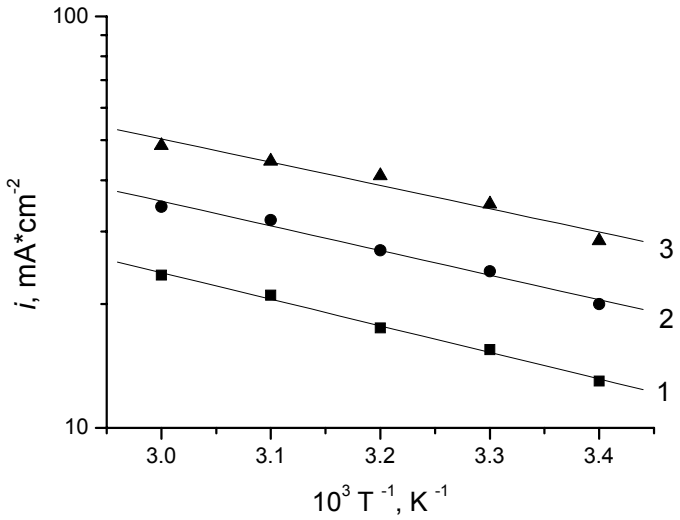

Fig. 5 – Plots of log i–1/T for HER on Ni in artificial seawater, at constant potentials: 1. – 1350; 2. – 1410; 3. – 1470 mV/SCE. Data in the Tafel region of the polarisation curves from Fig. 3.

Table 4

Arrhenius parameters for the HER on Ni in artificial seawater depending on the electrode potential

Potential, mV/SCE	- 1350	- 1410	-1470
Q, kJ/mol	12.37	11.46	10.66
i, A·cm^{-2}	2.04	2.19	2.51

The electrochemical impedance spectra in the complex plane, as Nyquist diagram and Bode plot, recorded at various potentials for Ni electrode, are shown in Fig. 6 and Fig. 7, respectively.

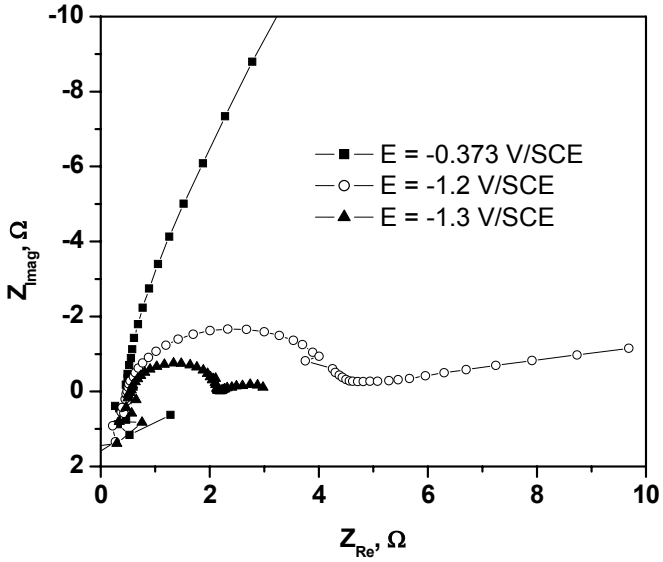

Fig. 6 – Nyquist diagrams for the HER on Ni electrode in artificial seawater, recorded at temperature of 25°C and various potentials.

At open circuit potential (OCP) of –0.373 V/SCE, the impedance data do not have a shape of a semicircle in the Nyquist plot (Fig. 6), suggesting a high value of corrosion resistance of Ni in artificial seawater, as shown previously.[2] The Bode plot (Fig. 7) also suggests a capacitive behaviour of the Ni electrode at OCP. The logarithm of impedance modulus ($\log|Z|$) has a linear variation with frequency logarithm (log f) having a slope of –0.82, which is close to the theoretical value of –1 for a pure capacitor. The phase angle (ϕ) is about 75° over a wide frequency range. Under these conditions, the parameter $|Z|$ is related to the double – layer capacitance, C_{dl}, as follows:

$$\log|Z| = \log\omega - \log C_{\mathrm{dl}} \qquad (7)$$

where the angular frequency is: $\omega = 2\pi \cdot f$. For $\omega = 1, f = 0.16$ Hz, $|Z|$ becomes equal to $1/C_{dl}$.

The value of C_{dl} at the OCP obtained from Fig. 6 is 0.31 mF·cm^{-2}. This value is much higher than the C_{dl} for Hg/solution interface (about 20 μF·cm^{-2}). Similar to the present study, high values of C_{dl} are reported for solid electrodes, such as Ni,[10] Ni–Zn alloy[19] and $Zr_{0.5}Ti_{0.5}V_{0.6}Cr_{0.2}Ni_{1.2}$ alloy[7] in alkaline solutions. It is assumed that these high values of C_{dl} are due to a pseudo-capacitance, which arises due to the adsorption of O_2, OH^- or intermediates of corrosion and passivation reactions at the solid electrode/electrolyte interface.

In the potential range of the hydrogen evolution reaction (more cathodic than –1.2 V/SCE), the Nyquist plots show well defined semicircles, that clearly indicates a charge transfer process on the Ni electrode. It was reasonably assumed that, in potential region where the Tafel line is obtained, the kinetics of the HER on Ni electrode are charge transfer controlled. Therefore, it was expected that the electrochemical impedance spectroscopy (EIS) would provide data consistent with the steady-state measurements. The appearance of a Warburg component, that is specific to a diffusion control, may be also observed on Nyquist diagrams at the potentials of –1.2 and –1.3 V/SCE. The similar behaviour of the HER

on Ni electrode is shown in Bode diagrams (Fig. 7); the phase angle is about –45°, specific to a diffusion control of the HER. The EIS data suggest that, in this potential region, the Tafel step may be the rate-determining step of the reaction, due to the slow diffusion of H_{ads} atoms to form H_2 molecule (reaction 3).

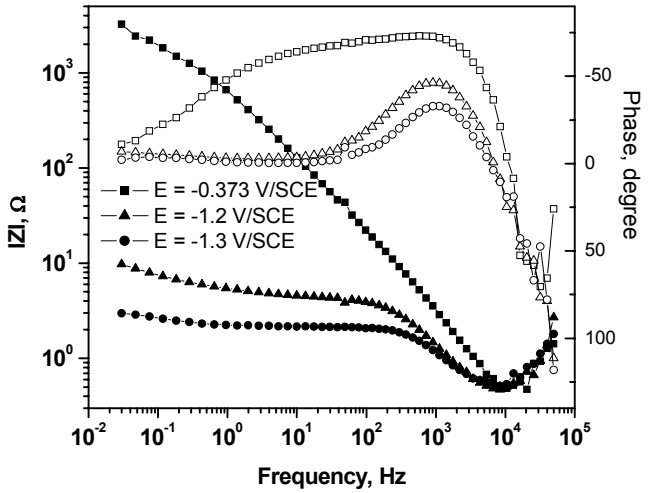

Fig. 7 – Bode diagrams at Ni electrode in artificial seawater at 25°C.

The EIS parameters of the Ni electrode in artificial seawater at 25°C are given in Table 5 depending on the potential.

Table 5

Experimental EIS parameters of Ni electrode in artificial seawater at 25°C at various potentials

Potential, V/SCE	– 0.373	– 1.200	– 1.300
R_s , Ω	0.45	0.48	0.51
R_{ct} , Ω·cm^2	-	9.6	4.9
C, mF·cm^{-2}	0.31	31	73

The significant increase of the capacitance at the potentials situated in the region of HER, similar with those reported by Rodrigues *et al.*[7], is due to the increase of the coverage by H_{ads} with shifting of potential in the negative direction.

As it was expected, the charge transfer resistance, R_{ct}, for HER decreases by cathodic polarisation. Thus, at the potential of –1.3 V, R_{ct} is about half of the value from –1.2 V/SCE (Table 5).

CONCLUSIONS

The interpretation of the kinetics data for the hydrogen evolution reaction (HER) obtained on Ni electrode in artificial seawater leads to the following conclusions:

The nickel is corrosion resistant both in the open circuit and by polarizing in the cathodic potential region.

The Tafel slope of the HER is significantly higher than –120 mV/decade and the corresponding charge transfer coefficient is lower than 0.5, indicating an important role of the adsorption processes in the reaction kinetics.

The exchange current density is of the same magnitude order (10^{-5}A·cm^{-2}) as the values reported in literature for HER on Ni in alkaline solutions.

The Tafel slope increases with temperature of solution whereas the charge transfer coefficient decreases.

The exchange current density and, therefore, the reaction rate of the HER increase with temperature. At 60°C, the value of i_0 is about 20 times more than that of 20°C.

In the Tafel region the energy of activation for HER has moderate values.

The EIS data show a capacitive behaviour of the Ni electrode in seawater at the open circuit potential. By polarizing at potentials more cathodic than –1.2 V/SCE, the Nyquist and Bode diagrams indicate a process controlled by charge transfer step (Volmer step) and by mass transfer of the

intermediate reaction product H_{ads} on electrode surface to combine in H_2 molecules (Tafel step).

REFERENCES

1. S. Trasatti, "Advances in Electrochemical Science and Engineering", H. Gerisher and C. W. Tobias, Eds., Weinheim: VCH, **1992**, vol. 2, p. 2.
2. I. Maior, G. E. Badea, A. Cojocaru and T. Badea, *Procedings of the 5th International Conference URB-CORR*: Study and Control of Corrosion in the Perspective of Sustainable Development of Urban Distribution Grids, May 18-20, 2006, Târgu Mureş, Roumania, Printech Bucharest, **2006**, p. 167.
3. N. Krstajić, M. Popović, B. Grgur, M. Vojnović and D. Šepa, *J. Electroanal. Chem.,* **2001**, *512*, 16.
4. N. Krstajić, M. Popović, B. Grgur, M. Vojnović and D. Šepa, *J. Electroanal. Chem.,* **2001**, *512*, 27.
5. C. Hitz and A. Lasia, *J. Electroanal. Chem.,* **2001**, *500*, 213.
6. J. R. C. Salgado, M. H. S. Andrade, J. C. P. Silva and J. Tonholo, *Electrochim. Acta,* **2002***, 47*, 1997.
7. C. Rodriguez, N. Munichandraiah and A. K. Shukla, *Bull. Mater. Sci*., **2000**, *23*, 389.
8. N. V. Krstajić, B. N. Grgur, N. S. Mladenović, M. V. Vojnović and M. M. Jakšić, *Electrochim. Acta*, **1997**, *42*, 323-330.
9. B. Losiewicz, A. Budniok, A. Lasia and E. Lagiewka, *Polish J. Chem.,* **2004**, *78*, 1457-1476.
10. L. Chen and A. Lasia, *J. Electrochem. Soc*. **1991**, *138*, 3321.
11. N. Spătaru, J-G. Lehelloca and R. Durand, *J. Applied Electrochem*., **1996**, *26*, 397.
12. R. Notoya, *Electrochim. Acta*, **1997**, *42*, 899.
13. G. Kreysa, B. Hakansson and P. Ekdunge, *Electrochim. Acta,* **1988**, *33*, 1351.
14. J. P. Diard, B. LeGorrec and S. Maximovitch, *Electrochim. Acta*, **1990**, *35*, 1099.
15. J. Tamm, L. Tamm and J. Arol'd, *Russ. J. Electrochem*., **2004**, *40*, 1152-1155.
16. B. C. Pound, "Modern Aspects of Electrochemistry", J. O'M. Bockris and B. E. Conway Eds., Plenum Press, New York, 1993, vol. 25, p. 63.
17. M. Julia, J. Ferreira and M. Da Cunha Belo, *Portugal. Electrochim. Acta,* **2004**, *22,* 263.
18. B. E. Conway, "Modern Aspect of Electrochemistry", B. E. Conway, R. E. White (Eds.), Plenum Press, New York, 1974, vol. 16, p.103.
19. H. Dumont, P. Los, A. Lasia, H. Menard and L. Brossard, *J. Applied Electrochem.,* **1993**, *23*, 684.